Fast Events in Protein Folding: Helix Melting and Formation in a Small Peptide[†]

Skip Williams,[‡] Timothy P. Causgrove,[§] Rudolf Gilmanshin,[||,⊥] Karen S. Fang,[‡] Robert H. Callender,[||] William H. Woodruff,[‡] and R. Brian Dyer*[,‡]

CST-4, Mail Stop J586, Los Alamos National Laboratory, Los Alamos, New Mexico 87545, Division of Science and Mathematics, P.O. Box W-100, Mississippi University for Women, Columbus, Mississippi 39701, and Department of Physics, City College of The City University of New York, New York, New York 10031

Received September 15, 1995; Revised Manuscript Received November 22, 1995[⊗]

ABSTRACT: The helix is a common secondary structural motif found in proteins, and the mechanism of helix−coil interconversion is key to understanding the protein-folding problem. We report the observation of the fast kinetics (nanosecond to millisecond) of helix melting in a small 21-residue alanine-based peptide. The unfolding reaction is initiated using a laser-induced temperature jump and probed using time-resolved infrared spectroscopy. The model peptide exhibits fast unfolding kinetics with a time constant of 160 ± 60 ns at 28 °C in response to a laser-induced temperature jump of 18 °C which is completed within 20 ns. Using the unfolding time and the measured helix−coil equilibrium constant of the model peptide, a folding rate constant of approximately 6×10^7 s^{-1} ($t_{1/2} = 16$ ns) can be inferred for the helix formation reaction at 28 °C. These results demonstrate that secondary structure formation is fast enough to be a key event at early times in the protein-folding process and that helices are capable of forming before long range tertiary contacts are made.

The question of how proteins fold from a random coil or quasi-random state to their final compact biologically active state (native state) is under intense theoretical and experimental investigation. It is evident that the native structure of the protein is coded within the primary amino acid sequence, but the fundamental physical and chemical processes which drive the sequence to a specific three-dimensional structure are not known. The folding process must somehow be guided, however, since a random search through all possible final states that the amino acid sequence might adopt to find the correct native state would take a very long time, certainly longer than the lifetime of an organism [the Levinthal paradox; see e.g. Creighton (1992) for a comprehensive review of the folding problem]. Because the precise structure of the folded protein is specifically linked to its biological activity, the protein-folding problem bears directly on practical issues, including structure−function relationships and the rational design of new proteins.

It has been known for about thirty years that many proteins will spontaneously unfold or fold reversibly in response to denaturing or renaturing conditions. A major stumbling block in experimental studies of protein-folding dynamics, however, is that these studies have generally employed techniques limited to millisecond or longer times and that key events occur faster than the millisecond time scale. In experiments based on the rapid mixing of solutions, for example, the reversibly denatured, unfolded protein in solution (e.g. at high concentrations of urea, extremes of pH, etc.) is rapidly diluted or mixed with reagents which reverse the denaturing conditions and chemically initiate folding. The best temporal response of studies based on mixing is typically one millisecond, the "dead time" of a stopped-flow apparatus, and the early events simply cannot be observed. Relaxation methods such as temperature jump (induced by capacitive discharge), electric field jump, and resonant ultrasound that access time scales as short as several nanoseconds have been applied to study the helix−coil kinetics of homopolymers consisting of several hundred units (see Discussion). However, the structural assignment of the kinetics observed by these approaches is not straightforward because of interference from molecular reorientation, solvation, charge transfer reactions, and/or proton transfer reactions, depending on the method. New experimental approaches are needed to study protein folding on fast time scales.

Because the α-helix is a common structural motif in proteins, it is important to understand the folding process of the α-helix in detail as a step toward understanding how proteins arrive at their native structures. For example, it has been proposed that short range interactions along the polypeptide chain of a forming protein induce regions of secondary structure which then act as nucleating regions for further collapse, leading to native tertiary structure [see e.g. Karplus and Weaver (1994) and Kim and Baldwin (1990)]. While there has been progress in understanding the thermodynamics of the helix−coil transition (Chou & Scheraga, 1971; Rialdi & Hermans, 1966; Scholtz et al., 1991), less is known about the kinetics of this process. In this paper, we report the unfolding kinetics of a small 21-residue α-helical peptide, the so-called suc-F_S 21-peptide: Suc-AAAAA-$(AAARA)_3$A-NH_2 (Suc = succinyl, A = alanine, and R = arginine). This peptide is reported to be greater than 90% helical in water at temperatures near 0 °C by Lockhart and Kim (1992, 1993). This peptide, like all small helical peptides, unfolds over a relatively large temperature range,

[†] This work was supported by grants from Los Alamos National Laboratory, XL60 (W.H.W. and R.B.D.), the National Institutes of Health, GM53640 (R.B.D.), and the National Science Foundation, MCB-9417892 (R.H.C.).

* To whom correspondence should be addressed.

[‡] Los Alamos National Laboratory.

[§] Mississippi University for Women.

[||] City College of The City University of New York.

[⊥] On leave from the Institute of Mathematical Problems of Biology, Russian Academy of Science.

[⊗] Abstract published in *Advance ACS Abstracts,* January 1, 1996.

0006-2960/96/0435-691$12.00/0

but a temperature change of 20 °C is large enough to significantly perturb the helix−coil equilibrium. In what follows, the suc-F_S 21-peptide will be referred to simply as the F_S peptide.

Our general approach to the rapid initiation and characterization of folding reactions is to use temperature to unfold a protein or peptide and to monitor the resulting changes using IR spectroscopy. The changes in the infrared spectrum that accompany the process are first characterized by obtaining equilibrium Fourier transform infrared (FTIR) spectra as a function of temperature. A laser-induced temperature jump (T-jump) is then used to initiate the unfolding process rapidly, and the subsequent kinetics are monitored using time-resolved infrared (TRIR) spectroscopy. The sensitivity of vibrational spectroscopy to protein structure is well-documented. The amide I absorption band, arising primarily from the C═O stretching vibrations of the carbonyls of the polypeptide backbone, is a particularly good indicator of secondary structural changes because of its marked sensitivity to hydrogen bonding and to structure dependent vibrational coupling. The T-jump is accomplished using a short (ca. 10 ns or shorter) near-infrared pump pulse at a wavelength where water absorbs but where polypeptides do not. The laser energy is absorbed by the water, and the temperature in the laser interaction volume is rapidly increased, typically by 15−30 °C. Our approach provides the time resolution and structural specificity necessary for determination of the kinetics of the helix−coil transition. This approach is also generally applicable to the study of protein folding since the biologically active compact states of proteins are stable over a specific range of temperatures and will unfold at temperatures both higher and lower than the range of stability.

MATERIALS AND METHODS

Peptide. The lyophilized F_S peptide was obtained from Professor Peter S. Kim (Lockhart & Kim, 1992, 1993). The peptide was then dissolved in D_2O at a typical concentration of 2 mM and used without further purification. The peptide purity was ascertained by C_{18} reverse-phase high-performance liquid chromatography (HPLC) to be greater than 95%. CD and NMR measurements indicate that no peptide aggregates form at 2 mM concentrations (Lockhart & Kim, 1992, 1993). The degree of helicity of the peptide is nearly constant between pH 1 and 8 and for NaCl concentrations up to 4 M (Lockhart & Kim, 1993). The final pH* of the 2 mM F_S peptide solutions was typically 4.1 ± 0.4 (uncorrected for D_2O). Trifluoroacetic acid (TFA) from the purification procedure was present in these solutions at approximately 6 mM concentrations.

Temperature Jump Generation. An injection-seeded Nd:YAG laser, pulsed dye laser, and WEX frequency differencing module working in conjunction produce the pulse at 2 μm [10 ns full width at half-maximum (FWHM) pulse width] which is the source for the temperature jump. The wavelength of the T-jump pulse corresponds to the peak of a weak D_2O near-IR absorption band ($\epsilon = 10.1$ cm^{-1} at 2 μm) and was chosen because 80% of the light is transmitted through 100 μm path length cells. The high transmission ensures a nearly uniform temperature profile in the approximately 9 nL ($300 \times 300 \times 100$ μm^3) laser interaction volume. In addition, this frequency is ideal for our purposes because most peptides and proteins do not absorb near 2 μm (5000 cm^{-1}). The laser energy is absorbed by the water (D_2O), and the temperature of the volume of water reaches its maximum value in approximately 20 ns (twice the FWHM of the pump pulse), since temperature thermalization and diffusion within water occur on subnanosecond time scales (Anfinrud et al., 1989; Genberg et al., 1987). The size of the T-jump was calibrated using the change of D_2O absorption with temperature which acts as an internal thermometer in the range of 1632−1700 cm^{-1}. Static measurements of the IR absorption of D_2O as a function of temperature yielded a nearly linear change in absorption with temperature at each wavelength. There is a small frequency dependence over the amide I absorption region with values ranging from 3.0×10^{-5} to 4.0×10^{-5} optical density (OD)/°C·μm for 1700 and 1632 cm^{-1}, respectively. The size of the temperature jump can be determined within 2 °C for each experiment. Temperature jumps of 18 °C are routinely obtained with this apparatus using 2 mJ of laser energy at 2 μm. The diffusion of heat out of the interaction volume takes several milliseconds in our cells. Thus, the apparatus generates a temperature jump within 20 ns that remains nearly constant up to approximately 1 ms.

Infrared Spectroscopy. The static infrared spectra were obtained using a Bio-Rad model FTS 60A FTIR spectrometer. Cryogenic copper cells employing 50−150 μm Teflon dual compartment (sample and reference) spacers and 25.4 × 2 mm CaF_2 windows were temperature controlled by a water bath with ±0.1 °C stability. A D_2O background spectrum was obtained under identical conditions (temperature, path length, and purge conditions) using the split cell and was subtracted from each peptide solution spectrum. The IR spectrum of D_2O contains a temperature dependent band near 1565 cm^{-1}, and subtraction of a reference spectrum of D_2O at each temperature is essential. The equilibrium FTIR spectra were found to be fully reversible, with results from either heating or cooling being identical. The reversibility of the IR results indicates that no peptide aggregation occurs at 2 mM concentrations.

The fundamental aspects of the transient IR spectrometer have been previously described (Causgrove & Dyer, 1993), and the details of the modifications required to perform temperature jump experiments is the topic of a future publication. In brief, the apparatus is capable of resolving real-time, single-wavelength infrared absorbance transients from 10 ns to arbitrarily long times (typically 25 ms) in one laser shot. A continuous wave (CW) lead salt infrared diode laser functions as the probe which is tunable from 1700 to 1632 cm^{-1}. Transient changes in the transmission of the CW IR beam through the sample are detected by a HgCdTe detector, digitized, and signal averaged (9000 shots at 10 Hz). The response function of the instrument has been improved by incorporation of a faster (50 MHz) detector/preamplifier system. The combined total instrument response time is approximately 23 ns which is currently limited by the detector/preamplifier system. A split IR cell was employed, one compartment containing D_2O plus peptide and the other containing D_2O. The cell was translated so that each compartment was probed under identical conditions. When D_2O is placed in both compartments, the measured transient absorbances are identical to within 10^{-3} OD which is approximately 10% of the maximum F_S peptide signal.

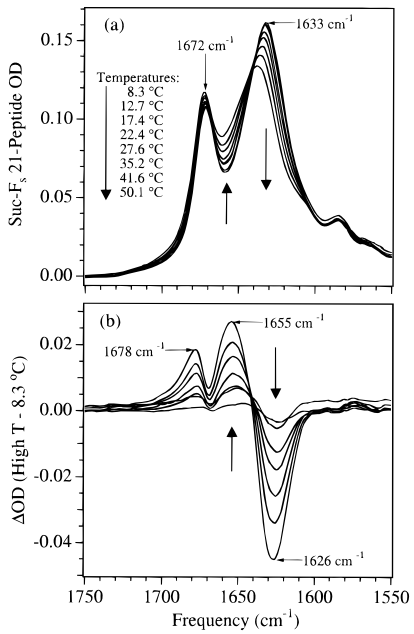

FIGURE 1: (a) FTIR spectra of a 2 mM F_s peptide solution in D_2O at pH* of 4.1 as a function of temperature. The D_2O background spectrum at each temperature is subtracted. The peak at 1633 cm^{-1} is the peptide amide I′ band, and the peak at 1672 cm^{-1} is due to TFA (see the text). (b) Difference FTIR spectra of F_s peptide generated by subtraction of the lowest temperature (8.3 °C) spectrum in (a) from spectra at higher temperatures. In (a) and (b), the arrows indicate the direction of spectral changes with increasing temperature. The path length for the equilibrium FTIR measurements is 140 μm.

RESULTS

Equilibrium FTIR spectra of the F_S peptide in the amide I′ spectral region as a function of temperature between 8.3 and 50.1 °C are shown in Figure 1a (the prime in amide I′ indicates a deuterated amide group). The major peak centered at 1633 cm^{-1} is the collective amide I′ absorbance of the main chain peptide groups. The smaller and sharper peak at 1672 cm^{-1} is the asymmetric carboxylate stretch of TFA ion which is present in these samples at approximately 6 mM concentrations. The amide I′ peak diminishes in intensity while broadening to retain approximately the same integrated intensity and shifts to higher frequency as the temperature is increased. The TFA peak shifts slightly to higher frequency as the temperature is increased. The amide I′ changes are consistent with CD measurements of helix melting in this temperature range (Lockhart & Kim, 1993). The broadening of the amide I′ absorption band is primarily due to an increased inhomogeneity resulting from a larger distribution of peptide conformers as the low temperature helical structure melts. The shift of the amide I′ absorption band to higher frequency is influenced by both the disruption of the relatively strong intrahelix hydrogen bonds with the concomitant formation of slightly weaker hydrogen bonds to water and the conformationally dependent changes in vibrational coupling.

Difference FTIR spectra are generated by subtraction of the lowest temperature (8.3 °C) spectrum from spectra at higher temperatures in Figure 1a. The difference spectra up to 50.1 °C are shown in Figure 1b. The positive and negative features shown in the figure are due to solute features which change with temperature and, as noted above, are indicative of structural differences between the folded and unfolded forms of the peptide. Specifically, the negative 1626 cm^{-1} feature in the difference spectra corresponds to a decrease of population of the low-temperature (folded helical) form of the peptide, and the positive 1655 cm^{-1} feature in the difference spectra corresponds to an increase of population of the high-temperature (unfolded coil) form. Note that these difference features result from populations shifting from a relatively narrow band centered at 1633 cm^{-1} to a much broader band centered at 1665 cm^{-1}. The positions of the two bands are somewhat temperature sensitive and shift to higher frequency with increasing temperature. The negative and positive features at 1670 and 1678 cm^{-1}, respectively, are due to the small shifts of the TFA carboxylate absorption.

The amide I′ mode arises predominately from polypeptide carbonyl C═O stretching vibrations. In general, when a proton donor hydrogen bonds to a carbonyl, as in the case of the peptide backbone C═O group in the helix conformation, electron density is drawn out of the C═O bond. This electron-withdrawing effect weakens the C═O force constant and lowers its stretching frequency. In addition, coupling among amide C═O oscillations in an extended structure is dependent on the nature of the structure. More precisely, the conformation of the main chain backbone of a polypeptide affects the observed frequency of the amide vibrations because the various motions of the peptide structure (primarily the C═O stretch, the C−N stretch, and the NH wag) couple with one another via dipolar, electronic, and kinematic mechanisms that are conformationally dependent [see e.g. Krimm and Bandekar (1986)]. Consequently, the frequency and width of the amide I′ band is sensitive to secondary structural changes, and empirical relationships between these observables and secondary structure in proteins have been assigned. For example, the amide I′ frequency of an α-helix in a folded protein occurs around 1655 cm^{-1}. Nevertheless, exceptions to these empirical rules exist, and the rigorous assignment of protein amide I′ subbands from equilibrium FTIR spectra to specific secondary structural elements is currently an active area of research [see e.g. Dong et al. (1990, 1992), Haris and Chapman (1992), Prestrelski et al. (1992), Surewicz and Mantsch (1988), Surewicz et al. (1993, and Susi and Byler (1986)].

In contrast, the assignment of empirical marker bands to specific secondary structure for small peptides is much less clear. Studies suggest that short helical peptides yield vibrational marker bands for both the α-helix and the 3_{10}-helix at frequencies near 1637 cm^{-1} (Haris & Chapman, 1995; Martinez & Millhauser, 1995; Miick et al., 1992). Accordingly, it is not possible to determine from IR data alone the exact helical form that is present even though infrared measurements reliably reveal the presence of helical structure in short peptides. That is, while we can clearly observe helix melting and formation, we cannot distinguish between an α-helix and a 3_{10}-helix from the IR data. However, NMR studies on the F_S peptide indicate that the folded form of the peptide is predominantly α-helix (Lockhart & Kim, 1993).

The equilibrium FTIR data demonstrate the sensitivity of the amide I′ C═O stretches to the conformational changes that take place during the unfolding of the peptide. The disappearance of the helix contribution can be monitored at frequencies near 1632 cm^{-1}, and the appearance of the unordered contribution can be monitored at frequencies near 1665 cm^{-1}. In Figure 2a, the absorption at 1632 cm^{-1} from

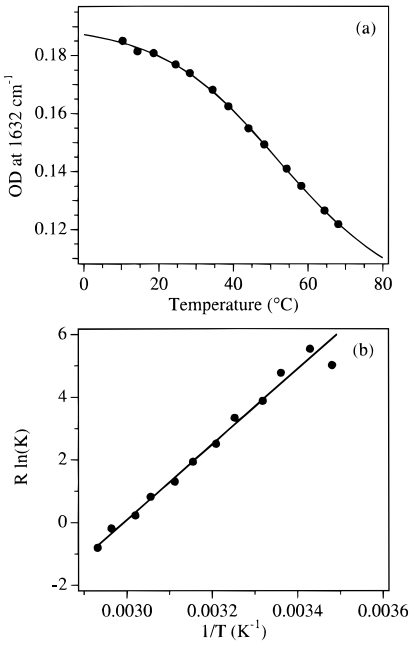

FIGURE 2: (a) Optical density (OD) at 1632 cm^{-1}, taken from data similar to that of Figure 1a, as a function of temperature and (b) a van't Hoff plot of these data (see the text for details of the fitting procedures used). The derived thermodynamic quantities for helix formation are $\Delta H_{vH} = -12 \pm 2$ kcal/mol (-0.6 ± 0.1 kcal/mol per residue), $\Delta S_{vH} = -36 \pm 6$ cal/mol·K, and an equilibrium constant of 10 ± 2 favoring helix formation at 27.4 °C.

the data similar to that of Figure 1a is plotted as a function of temperature. As is generally observed for small peptides, the helix−coil transition of the F_S peptide takes place over a relatively broad temperature range, indicating that the transition is weakly cooperative. The F_S peptide is known to be greater than 90% helical in water at temperatures near 0 °C [see e.g. Lockhart and Kim (1992, 1993)], and this is consistent with the high IR absorption at 1632 cm^{-1} at low temperatures. However, considerable absorption at 1632 cm^{-1} is observed even at the very highest temperatures where CD measurements (Lockhart % Kim, 1993) indicate that the peptide is unfolded. The absorption data as a function of temperature in Figure 2a were fit to a functional form derived for the helix−coil transition for peptides assuming a two-state system [page 236 of Hoppe et al. (1983)]. The solid curve through the data points in Figure 2a is the result of this fit, and a melting temperature, T_M, of 61 °C was obtained. The van't Hoff plot derived from this fit to the data is shown in Figure 2b, where the log of the equilibrium constant is plotted versus $1/T$. The relevant thermodynamic parameters for helix formation obtained from a linear regression analysis of the data plotted in Figure 2b are $\Delta H_{vH} = -12 \pm 2$ kcal/mol (-0.6 ± 0.1 kcal/mol per residue), $\Delta S_{vH} = -36 \pm 6$ cal/mol·K, and an equilibrium constant of 10 ± 2 favoring helix formation at 27.4 °C. The errors in the thermodynamic parameters are based on an estimate of the uncertainty in the background absorption at 1632 cm^{-1} and from run-to-run variations in the values.

Amide I′ transient absorption changes resulting from a T-jump from 9.3 to 27.4 °C in a sample of the F_S peptide in D_2O are shown in Figure 3. We are able to distinguish the transient absorption changes of the F_S peptide despite the fact that most of the absorption changes are due to a very fast change in the broad mid-IR absorption background of D_2O with temperature (right vertical axis). Consequently,

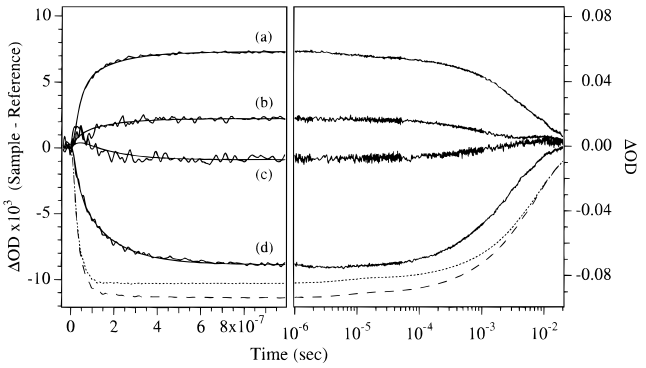

FIGURE 3: Change in optical density (ΔOD) at 1632 cm^{-1} of D_2O (reference, dotted line) and the F_s peptide in D_2O (sample, dashed line), right vertical axis, and change in optical density (ΔOD) of sample minus reference at (a) 1655 cm^{-1}, (b) 1664 cm^{-1}, (c) 1637 cm^{-1}, and (d) 1632 cm^{-1}, left vertical axis, as a function of time in response to a temperature jump from 9.3 ± 1 to 27.4 ± 2 °C. Conditions are the same as those described in the legend to Figure 1a. The solid curves represent fits of the data to biexponential kinetics convoluted with the instrument response function determined from the D_2O reference transient absorption data. The two components of the biexponential model have time constants of <10 ns (instrument limited) and 160 ± 60 ns and relative amplitudes ranging from 0.9 to 1.9. The path length for the TRIR kinetic measurements is 110 μm.

extreme care must be taken to subtract the large D_2O contribution from the transient absorption data. The subtraction error is minimized in these experiments by using a split cell having a sample and reference compartment which are precisely matched in path length and temperature as described in the Materials and Methods. The D_2O reference transient absorption data shown in Figure 3 are instrument limited by the 50 MHz bandwidth of the infrared detector/preamplifier system. The combined instrument response of this system is 23 ns as determined by modeling the D_2O reference signal. Therefore, with this system, we can measure transients with time constants of approximately 10 ns or longer.

The difference signals between the D_2O reference and the F_S peptide in D_2O solution are shown in Figure 3 at (a) 1655 cm^{-1}, (b) 1664 cm^{-1}, (c) 1637 cm^{-1}, and (d) 1632 cm^{-1} (left vertical axis). As can be seen in the figure, a relatively modest temperature jump of 18 °C produces a change in the folded population that is easily detected with the sensitivity of our TRIR apparatus. The solid curves are fits of the data to a double exponential kinetic model convoluted with the instrument response. All the kinetic traces were fit using the same two time constants, but the relative amplitudes of the two components varied from 0.9 to 1.9 depending on the wavelength. The first time constant is instrument limited (<10 ns), and the second time constant is 160 ± 60 ns. Because all the data can be fit with the same two time constants, the production of the unordered form of the peptide occurs on the same time scale as the depletion of the helix form. The decay of the transient absorption changes at longer times is due to the millisecond decay of the temperature in the laser interaction volume (see the D_2O reference transient data of Figure 3). Because the F_S peptide transient absorption data follow the millisecond decay of D_2O reference data, i.e. the millisecond decay of the temperature, the peptide must refold on submillisecond or faster time scales. The folding kinetics are discussed in more detail in the following section.

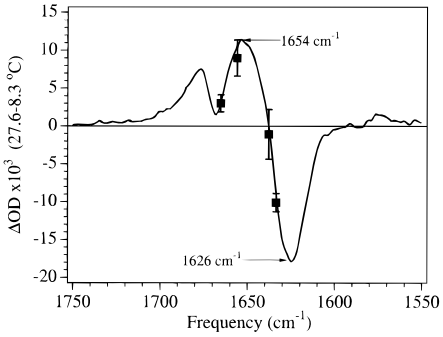

FIGURE 4: Comparison of the 27.6 − 8.3 °C FTIR difference spectrum (solid line) to the 1 μs transient absorption spectrum (symbols) for the F_s peptide. The transient spectrum was obtained from the magnitude of transient absorption data (sample minus reference) shown in Figure 3 taken at 1 μs. Note that the transient absorption data have been scaled to reflect the concentration and path length conditions of the FTIR data.

The magnitude of all the transient absorption data 1 μs after the T-jump is plotted against frequency in Figure 4 to create a high-minus low-temperature transient difference spectrum for the F_S peptide. The equilibrium FTIR difference spectrum for an equivalent temperature difference is also shown in Figure 4 for comparison. As in Figure 3, the experimental error arises primarily from the subtraction error associated with matching the sample and reference compartments. The 1 μs transient difference spectrum is the same within experimental error as the FTIR equilibrium spectrum which confirms that all of the structural changes observed in the FTIR equilibrium data are completed before 1 μs. Therefore, the kinetics of helix unfolding of the F_S peptide at 28 °C are described well by kinetic processes with time constants less than ca. 160 ns.

DISCUSSION

The variation of IR absorption bands with structural changes accompanying protein folding differs in detail from that of the more commonly used structure sensitive probes of folding such as CD or NMR. In particular, the signature of the helical structure detailed by CD requires an ordered helix to be present over relatively long distances, while the coupling phenomenon which modulates the amide I IR signature varies with the ϕ, ψ angles of adjacent amino acid residues as well as the hydrogen-bonding interactions resulting from a single turn of helix. Accordingly short, isolated segments of helical structure may be detected by IR but not by CD. In this sense, the two techniques are complementary [see also Guijarro et al. (1995) and Hirst and Brooks (1994)].

The equilibrium measurements of the amide I′ absorption band as a function of temperature are in qualitative agreement with unfolding studies of the F_S peptide performed using CD as the monitor (Lockhart & Kim, 1992, 1993); i.e. in both sets of measurements, the unfolding takes place over a broad temperature range. However, quantitative agreement is neither expected nor observed. For example, the CD studies yield a peptide melting temperature of 39 °C, whereas the IR results yield a melting temperature of 61 °C and show that a significant amount of helical structure is present even after "complete" melting, by CD criteria, has occurred. In addition, the IR results demonstrate that the unfolding of this peptide is not a simple two-state helix−coil transition. The lack of two-state equilibrium behavior is indicated by the absence of a sharp isosbestic point at zero in the FTIR difference spectra of Figure 1b. The relatively small unfolding enthalpy derived from the van't Hoff plot of Figure 2b also suggests non-two-state behavior. The enthalpy of helix formation in alanine-based peptides has been recently examined in some detail (Scholtz et al., 1991, and references therein). Helix formation is favored enthalpically and appears to be largely determined by main chain interactions (presumably involving the amide hydrogen bond and packing interactions). The calorimetric value of the enthalpy of helix formation, ΔH_{cal}, obtained from integration of heat capacity in differential-scanning calorimetry experiments gives a best estimate of −1.3 kcal/mol per residue, which is about twice the value found in the van't Hoff analysis of the F_S peptide thermal unfolding curves, ΔH_{vH}. It is always found that $\Delta H_{cal} > \Delta H_{vH}$ when a thermal transition as a function of temperature proceeds through intermediate forms (Cantor & Schimmel, 1980; Scholtz et al., 1991).

In principle, the helix−coil transition can involve various compact forms of the helix such as the α-helix and the 3_{10}-helix and various degrees of unfolding, for example, preferential unfolding of the ends of the peptide versus the middle (Shalongo et al., 1994). FTIR studies of the sort here are capable of addressing such questions since it is possible to synthesize peptides where individual residues are isotopically labeled. For example, the frequency of the amide I′ C═O stretch is downshifted by about 40 cm^{-1} by incorporation of ^{13}C═O, and this spectral shift allows contributions from specific residues to be identified. Such studies are now underway on the F_S peptide and will provide information regarding the degree of structural inhomogeneity of the unfolded state and whether different regions of the peptide unfold/fold at different rates. In addition, much work needs to be carried out to determine clear vibrational marker bands for distinct structures that might exist in peptides, such as the α-helix and the 3_{10}-helix. In advance of such detailed studies, however, it is informative to discuss the results in terms of a simple helix−coil transition, recognizing that this is not the case in detail.

The unfolding kinetics of the F_S peptide in response to a T-jump from 9.3 to 27.4 °C are described well by a biexponential model having components with time constants of ca. <10 and ca. 160 ns. One possible explanation of the faster component is that it results from a temperature-induced shift of the infrared absorption spectrum of the peptide which occurs in the absence of actual helix melting. This assignment is supported by the fact that the two component bands at 1633 cm^{-1} (folded form) and 1665 cm^{-1} (unfolded form) shift to higher frequency with increasing temperature. This frequency shift could result, for example, because of a difference in the solvation of the peptide at the higher temperature without change in the helical content [see e.g. Chen et al. (1994)]. Thus, we suggest that the actual unfolding process is described by the slower component. Furthermore, the slower unfolding time can be used with an equilibrium constant to estimate the folding rate. An equilibrium constant of 10 favoring helix formation at 27.4 °C is derived from the data of Figure 2 which yields an estimated (within 1 order of magnitude) folding rate constant of 6×10^7 s^{-1} ($t_{1/2}$ = 16 ns) for this peptide. Recently, Levitt and co-workers (M. Levitt, personal communication) have simulated the unfolding of a 13-residue alanine peptide in water using detailed interatomic force fields. They

observed that a temperature jump from 4 to 25 °C leads to the unfolding of this 13-residue peptide in a few nanoseconds. In addition, Sung and Wu (1995) have simulated the folding of a 12-residue alanine peptide from an extended structure and found that helix−coil equilibrium was achieved in 4 ns at 1 °C. The qualitative agreement of the simulations with our results is encouraging.

Several groups have used a variety of relaxation methods to study fast processes in long homopolymers (several hundred units), including, presumably, the helix−coil transition. These studies employed electric field jump (Cummigs & Eyring, 1975; Sano & Yasunga, 1980), temperature jump (Bosterling & Engel, 1979; Hamori & Scheraga, 1967; Lumry et al., 1964), and resonant ultrasound (Barksdale & Stuehr, 1972; Grunenewald et al., 1979; Hammes & Roberts, 1969; Inoue, 1970) to perturb the various equilibria, including the helix−coil equilibrium. Interpretation of the relaxation results in terms of helix−coil kinetics, however, is complicated by interfering phenomena, including molecular reorientation, solvation, charge transfer reactions, and/or proton transfer reactions, depending on the method. Nevertheless, experimentally observed relaxation times from 15 μs to 20 ns were assigned to the helix−coil transition in the long homopolymers, depending on the system and on the method. From these relaxation times, rate constants were inferred for the formation of a single turn of helix in the range of 1×10^7 to 7×10^{10} s^{-1} [see e.g. Gruenewald et al. (1979)]. The results of these studies are not inconsistent with our inferred folding rate constant of 6×10^7 s^{-1} for the small 21-residue alanine peptide. Furthermore, Hochstrasser and co-workers have recently observed nanosecond amide I′ absorbance transients in T-jump experiments perturbing the β-sheet structure of ribonuclease A (Phillips et al., 1995). Because of technical limitations, however, the unfolding kinetics were only followed out to approximately 3 ns and were not resolved.

An essential result of our study is that the folding kinetics of a short length of peptide, such as that found in proteins, can occur within a few tens of nanoseconds which is much shorter than the time scale of the formation of intramolecular tertiary contacts from one point of a polypeptide chain to another. Theoretical studies assuming that disparate lengths of protein come into contact with each other diffusely predict the time for a random collision between the two ends of a small protein like apomyoglobin to be approximately 5 μs or slower [see e.g. Karplus and Weaver (1979, 1994)]. The recent experimental studies on cytochrome *c* (Jones et al., 1993), where photodissociation of CO bound to the heme site of the unfolded protein initiates the folding reaction, suggest that the native contacts between the heme prosthetic group with its methionine ligand are reestablished in 40 μs. Therefore, the characteristic time scale of helix formation would appear to be some 3 orders of magnitude faster than the characteristic time scale of intramolecular tertiary contact formation.

The protein-folding process involves both short range and long range forces. For at least two decades, it has been hypothesized that elements of secondary structure of proteins are coded into the primary sequence and are early intermediates along the folding pathway [see e.g. Kim and Baldwin (1990)]. This hypothesis follows from the possibility that such conformations, either fully formed or in a nascent state, could serve as nucleation structures about which appropriate tertiary contacts are made. If this hypothesis is taken to its limit, the primary sequence is a code of crucial start and stop signals with appropriate residues in between for the specific elements of secondary structure required to bring about the proper folding of a particular protein. A random search over all possible conformations of an entire protein to find the lowest energy configuration (the Levinthal paradox) does not take place; rather, a search for secondary structure over small lengths of polypeptide is a key process at early times followed by searches for favorable tertiary contacts involving these sections of secondary structure at longer times. Hence, the folding process occurs in a reasonable time, because local interactions dominate the process at early times and directly affect the process at longer times. In support of this view, it has been shown that short peptide lengths of various native proteins adopt the correct or nearly correct secondary structure in aqueous solution or, in some cases, in solutions which promote secondary structure formation. The G and H α-helical runs as well as reverse and hairpin turns in apomyoglobin (Shin et al., 1993a,b; Waltho et al., 1993), the α-helical runs of ribonuclease (Kim & Baldwin, 1984, 1990; Udgaonkar & Baldwin, 1990), the α-helical runs of myohemerythrin (Dyson et al., 1992a), the α-helical runs of barnase (Kippen et al., 1994), and conformational preferences of extended β-structure of peptides derived from the β-sheet protein plastocyanin (Dyson et al., 1992b) are examples.

In contrast, other theoretical approaches to the folding problem which put secondary structure formation on a different footing with regard to its importance in folding have been developed. For example, Dill and co-workers suggest that hydrophobic collapse and the resultant compact states of proteins lead to the concomitant formation of secondary structure (Dill et al., 1995). It is also unclear how the forces responsible for secondary structure formation or the role of secondary structure formation itself are modeled in recent theoretical treatments of the energy landscape appropriate for proteins [see e.g. Wolynes et al. (1995)] or in dynamic models where the residues in a protein are simplified to self-interacting monomers, often on lattices, with a limited set of specific interactions [see e.g. Karplus and Sali (1995) and Sali et al. (1994)]. Our results suggest that these models need to incorporate specifically the formation of stable secondary structure at early times.

CONCLUSIONS

On the time scale of long range tertiary contact formation, the kinetics of the helix−coil interconversion are very rapid. Our results are thus in agreement with the notion that secondary structure forms first before long range tertiary contacts are made. Moreover, our results show that it is not necessary for a peptide sequence to have a strong propensity for helix formation in aqueous solution in order to serve as a nucleation site. This statement follows from the fact that the time scale of helix formation is so much faster than the time it takes for long range tertiary contacts to take place by diffusion that a trace concentration of the helix would be enough for nucleation, provided the tertiary interactions strongly favor the helix form over the coiled form. In this regard, experimental measurements of even trace formation of specific secondary structures associated with specific sequences of residues become quite meaningful.

ACKNOWLEDGMENT

We thank Professor P. S. Kim and Dr. D. J. Lockhart for kindly providing the F_s peptide.

REFERENCES

Anfinrud, P. A., Han, C., & Hochstrasser, R. M. (1989) *Proc. Natl. Acad. Sci. U.S.A. 86*, 8387−8391.
Barksdale, A. D., & Stuehr, J. E. (1972) *J. Am. Chem. Soc. 94*, 3334−3338.
Bosterling, B., & Engel, J. (1979) *Biophys. Chem. 9*, 201−209.
Cantor, C. R., & Schimmel, P. R. (1980) *Biophysical Chemistry. Part III: The Behavior of Biological Molecules*, W. H. Freeman & Co., San Francisco.
Causgrove, T. P., & Dyer, R. B. (1993) *Biochemistry 32*, 11985−11991.
Chen, X. G., Schweitzer-Stenner, R., Krimm, S., Mirkin, N. G., & Asher, S. A. (1994) *J. Am. Chem. Soc. 116*, 11141−11142.
Chou, P. Y., & Scheraga, H. A. (1971) *Biopolymers 10*, 657−680.
Creighton, T. E., Ed. (1992) *Protein Folding*, pp 1−547, W. H. Freeman & Co., New York.
Cummings, A. L., & Eyring, E. M. (1975) *Biopolymers 14*, 2107−2114.
Dill, K. A., Bromberg, S., Yue, K., Fiebig, K. M., Yee, D. P., Thomas, P. D., & Chan, H. S. (1995) *Protein Sci. 4*, 561−602.
Dong, A., Huang, P., & Caughey, W. S. (1990) *Biochemistry 29*, 3303−3308.
Dong, A., Huang, P., & Caughey, W. S. (1992) *Biochemistry 31*, 182−189.
Dyson, H. J., Merutka, G., Waltho, J. P., Lerner, R. A., & Wright, P. E. (1992a) *J. Mol. Biol. 226*, 795−817.
Dyson, H. J., Sayre, J. R., Merutka, G., Shin, H.-C., Lerner, R. A., & Wright, P. E. (1992b) *J. Mol. Biol. 226*, 819−835.
Genberg, L., Heisel, F., McLendon, G., & Miller, R. J. D. (1987) *J. Phys. Chem. 91*, 5521−5524.
Gruenewald, B., Nicola, C. U., Lustig, A., Schwarz, G., & Klump, H. (1979) *Biophys. Chem. 9*, 137−147.
Guijarro, J. I., Jackson, M., Chaffotte, A. F., Delepierre, M., Mantsch, H. H., & Goldberg, M. E. (1995) *Biochemistry 34*, 2998−3008.
Hammes, G. G., & Roberts, P. B. (1969) *J. Am. Chem. Soc. 91*, 1812−1816.
Hamori, E., & Scheraga, H. A. (1967) *J. Phys. Chem. 71*, 4147−4150.
Haris, P. I., & Chapman, D. (1992) *TIBS 17*, 328−333.
Haris, P. I., & Chapman, D. (1995) *Biopolymers 37*, 251−263.
Hirst, J. D., & Brooks, C. L., III. (1994) *J. Mol. Biol. 243*, 173−178.
Hoppe, W., Lohmann, W., Markl, H., & Ziegler, H. (1983) *Biophysics*, 2nd ed., pp 233−242, Springer-Verlag, Berlin.
Inoue, H. (1970) *J. Sci. Hiroshima Univ., Ser. A-2 34*, 37.
Jones, C. M., Henry, E. R., Hu, Y., Chan, C.-K., Luck, S. D., Bhuyan, A., Roder, H., Hofrichter, J., & Eaton, W. A. (1993) *Proc. Natl. Acad. Sci. U.S.A. 90*, 11860−11864.
Karplus, M., & Weaver, D. L. (1979) *Biopolymers 18*, 1421−1437.
Karplus, M., & Weaver, D. L. (1994) *Protein Sci. 3*, 650−668.
Karplus, M., & Sali, A. (1995) *Curr. Opin. Struct. Biol. 5*, 58−73.
Kim, P. S., & Baldwin, R. L. (1984) *Nature 307*, 329−334.
Kim, P. S., & Baldwin, R. L. (1990) *Annu. Rev. Biochem. 59*, 631−660.
Kippen, A. D., Sancho, J., & Fersht, A. R. (1994) *Biochemistry 33*, 3778−3786.
Krimm, S., & Bandekar, J. (1986) *Adv. Protein Chem. 38*, 181−364.
Lockhart, D. J., & Kim, P. S. (1992) *Science 257*, 947−951.
Lockhart, D. J., & Kim, P. S. (1993) *Science 260*, 198−202.
Lumry, R., Legare, R., & Miller, W. G. (1964) *Biopolymers 2*, 489.
Martinez, G., & Millhauser, G. (1995) *J. Struct. Biol. 114*, 23−27.
Miick, S. M., Martinez, G. V., Fiori, W. R., Todd, A. P., & Millhauser, G. L. (1992) *Nature 359*, 653−655.
Phillips, C. M., Mizutani, Y., & Hochstrasser, R. M. (1995) *Proc. Natl. Acad. Sci. U.S.A. 92*, 7292−7296.
Prestrelski, S. J., Byler, D. M., & Liebman, M. N. (1992) *Proteins: Struct., Funct., Genet. 14*, 440−450.
Rialdi, G., & Hermans, J., Jr. (1966) *J. Am. Chem. Soc. 88*, 5719−5720.
Sali, A., Shakhnovich, E., & Karplus, M. (1994) *Nature 369*, 248−251.
Sano, T., & Yasunga, T. (1980) *Biophys. Chem. 11*. 377−386.
Scholtz, J. M., Marqusee, S., Baldwin, R. L., York, E. J., Stewart, J. M., Santoro, M., & Bolen, D. W. (1991) *Proc. Natl. Acad. Sci. U.S.A. 88*, 2854−2858.
Shalongo, W., Dugad, L., & Stellwagen, E. (1994) *J. Am. Chem. Soc. 116*, 2500−2507.
Shin, H.-C., Merutka, G., Waltho, J. P., Wright, P. E., & Dyson, H. J. (1993a) *Biochemistry 32*, 6348−6355.
Shin, H.-C., Merutka, G., Waltho, J. P., Tennant, L. L., Dyson, H. J., & Wright, P. E. (1993b) *Biochemistry 32*, 6356−6364.
Sung, S.-S., & Wu, X.-W. (1995) in *Proceedings of the Protein Society Symposium*, Boston, pp 109.
Surewicz, W. K., & Mantsch, H. H. (1988) *Biochim. Biophys. Acta 952*, 115−130.
Surewicz, W. K., Mantsch, H. H., & Chapman, D. (1993) *Biochemistry 32*, 389−394.
Susi, H., & Byler, D. M. (1986) *Methods Enzymol. 130*, 290−311.
Udgaonkar, J. B., & Baldwin, R. L. (1990) *Proc. Natl. Acad. Sci. U.S.A. 87*, 8197−8201.
Waltho, J. P., Feher, V. A., Merutka, G., Dyson, H. J., & Wright, P. E. (1993) *Biochemistry 32*, 6337−6347.
Wolynes, P., Onuchic, J. N., & Thirumalai, D. (1995) *Science 267*, 1619−1620.

BI952217P